ASTRONOMY & ASTROPHYSICS
SUPPLEMENT SERIES

Astron. Astrophys. Suppl. Ser. **120,** 57-61 (1996)

Grids of pre-main sequence stellar models. The accretion scenario at Z=0.001 and Z=0.020

P.A. Bernasconi

Observatoire de Genève, CH-1290 Sauverny, Switzerland
email: paolo.bernasconi@obs.unige.ch

Received February 12; accepted April 5, 1996

Abstract. — I present and briefly discuss a new set of pre-main sequence (MS) evolutionary tracks computed in the framework of the accretion paradigm for star formation at metallicities Z=0.001 and Z=0.020. Improved birthlines are obtained from a time-dependent prescription for the accretion rate. These evolutionary sequences are better suited than the canonical approach which starts arbitrarily high on a luminous Hayashi adiabat, to interpret color-magnitude diagrams and ages of young stellar associations. They also constitute a (both physical and numerical) self-consistent extension to the post-MS stellar models previously published by the Geneva group (Schaller et al. 1992).

Key words: stars: evolution — stars: pre-main sequence — Hertzsprung-Russel (HR) diagram

1. Introduction

Adopting model atmospheres, one is enabled to relate color-magnitude plots to synthetic Hertzsprung-Russell diagrams (HRD), and extrapolate valuable informations like ages, masses or initial mass functions to whole photometric samples of known metallicities. However, this strategy demands the following points to be strictly satisfied: 1) On observational grounds, the collected fluxes must refer to the naked photospheric properties of single stars. It is up to the observers to subtract any non-stellar luminosity excesses from the original data, should these components affect the optical spectra; 2) Evolutionary tracks must prove as much as possible insensitive to the precise internal structure of the starting configuration. Otherwise, we can only hope (or demonstrate, if possible) that its initial properties are sufficiently well constrained by the prevailing physical processes operating at previous times, to add only marginal uncertainties on the derived stellar parameters.

In post-MS computations the second requirement has always been tacitely assumed, and except perhaps for the higher mass stars which totally lack for an optically recognizable pre-MS stage (Bernasconi & Maeder 1996, BM hereafter), there are no serious reasons to question it. Both warnings however are of the utmost importance when trying to interpret HRDs of star forming regions.

In the optically shrouded formation stage first, and during part of their early pre-MS evolution, low and intermediate mass stars strongly interact with their circumstellar environment. An extended period of mass accretion through the inner boundary of a geometrically thin accretion disk seems an inevitable consequence of the collapse of self-gravitating, rotating clouds marginally unstable to the Jeans (or Bonnor-Ebert) criterion (Larson 1969; Tscharnuter 1991). The most difficult task then consists in predicting the boundary conditions at the photosphere of an accreting core, since the amplitude of the entropy input and viscous or magnetic torques acting upon it can appreciably modify the evolutionary track followed by a young star of given final mass M (Mercer-Smith et al. 1984; Martin & Claret 1996). As a matter of fact, the absence of even an approximate correspondence between spectrophotometric properties and luminosity (or age) within homogeneous mass samples on their convective sequences, supports the belief that stars of identical zero age MS (ZAMS) mass can be formed, starting from moderately different initial properties for their respective parental molecular clouds (Basri et al. 1991; Bouvier et al. 1993).

Even bounded to the preceding few considerations, we are tempted to assert that the task of correcting the photometric fluxes from any circumstellar emission activity linked to the formation process, should not compete to observers (they would anyhow need to model the underlying cause), but should be the aim of a complete theory of star formation to integrate all pertinent components (like disks) into a coherent theoretical picture and to provide a better astrophysical tool other than HRDs to interpret less ambiguously the observational data (Palla 1996). Meanwhile, first order effects give already considerable

improvements with respect to the canonical scenario to deserve the earnest attention. In this regard, the present paper offers new grids of pre-MS evolutionary tracks computed in the framework of the accretion scenario as developed for low and intermediate mass stars by Stahler 1983 and Palla & Stahler (1991, 1993), and tentatively extended to treat the formation stage of higher mass stars by BM. These calculations represent the subsequent logical step of the work started by BM. They are also intended as a comparison basis for future work including rotation and residual mass accretion (in preparation), as well as an extension of the accretion scenario to relevant metallicities not yet considered in the literature.

2. Input physics

At a typical isothermal ($\sim$ 30 K), namely constant accretion rate of 10^{-5} $M_\odot$ yr^{-1} and interstellar deuterium mass fraction of a few 10^{-5}, deuterium burning alone is not in position to halt the quasi-static contraction of an accreting core. However, the Kelvin-Helmholtz timescale for a $0.01-0.4$ $M_\odot$ core is so high, that even a partial thermostatic support will determine the stellar configuration to stay about the deuterium MS (DMS). As a starting model then, we confidently opted for a 0.7 $M_\odot$ fully convective polytrope at, or very near the DMS. This choice closely reproduces the accreted models of Stahler, which turn completely convective owing to deuterium ignition at a total stellar mass of 0.4 $M_\odot$. The further assumption of anisotropic accretion weakens the strength of the optically thin shocked layer near the equator, allows the converted mechanical and gravitational energies to freely leave the system as radiation, and legitimizes the use all along the main accretion phase of standard photospheric boundary conditions.

The newly accreted deuterium is instantaneously mixed within the convective envelope (see however BM). Relaxing this hypothesis, i.e. using a time dependent diffusive approach, is globally irrelevant, though it can modify the predicted surface abundances of the light isotopes.

The time history of the accretion rate is computed from the turbulent solution of BM for isolated massive stars, and is supposed not to depend on the final stellar mass. It rests on a model for spherically symmetric cloud cores supported by the joined action of a thermal component slightly metallicity-dependent, and a turbulent (locally isotropic), metallicity-independent component which account for the observed power law relation $\sigma_{\rm NT} = ar^m$, $0.3 < m < 0.7$, linking the nonthermal, molecular linewidths $\sigma_{\rm NT}$ to the size r of the cloud (Larson 1981). Its magnitude is monotonically increasing, and varies between 1 and $\sim$ 2.5 10^{-5} $M_\odot$ yr^{-1} for the earlier B stars. The photospheric properties of successive accretion models define an upper boundary for the optical appearence of pre-MS stars (the *birthline*). From there on, the models are followed during their final approach to the ZAMS in the standard manner and employing the same physics as described in BM (Appendix).

We made use of the OPAL relative metal abundances (Iglesias et al. 1992), except for the fragile, primordial elements ^{2}H, ^{3}He, ^{6}Li and ^{7}Li whose interstellar medium (ISM) mass fractions are set at 3.4 10^{-5}, 5.1 10^{-5}, 8.6 10^{-10}, 1 10^{-8}, and at 3.8 10^{-5}, 5.7 10^{-5}, 1.4 10^{-10}, 1.6 10^{-9} for the Z=0.020, Z=0.001 grids, respectively (Boesgaard & Steigman 1985; Geiss 1993). Radiative opacities are from Iglesias & Rogers (1993) completed at low temperatures with the atomic and molecular opacity tables of Kurucz (1991).

3. Short discussion of the main results

In this section we shall summarize the most prominent features of the grids, deferring a thorough discussion of the effects of rotation, time dependent deuterium mixing and residual mass accretion to a forthcoming paper.

Birthlines: The birthline for each metallicity is plotted as a thick line in Fig. 1. A number of relevant quantities are gathered in Tables 1 and 2. The core remains fully convective till a total mass of 2.43 $M_\odot$ for a metallicity Z=0.020 (1.98 $M_\odot$ at Z=0.001) and a central temperature of 5.0 10^6 (4.0 10^6) K, where an off-center radiative barrier marks its return to radiative equilibrium. The convective envelope quickly shrinks to ultimately disappear after a mere 1.25 10^5 (7.86 10^4) yr, less than the radiative diffusion timescale, at a core mass of 4.24 (3.08) $M_\odot$, so that the core appears underluminous for its actual mass. However, an ascending luminosity front is not late in bursting out past the surface, swelling the external shells and leading the birthline to recover the narrow band in the HRD where pre-MS Herbig AeBe stars are actually found. This envelope is broadly defined by strong CO outflows sources (Palla & Stahler 1992). The accretion time equals the integrated contraction time at 8.40 (7.28) $M_\odot$, when the birthline eventually intercepts the ZAMS.

The shape of the birthline is mainly controlled by three factors, all directly or indirectly modified by changing the metallicity: the accretion rate (through its thermal part), the ISM deuterium mass fraction, and the stellar opacity. The first of these effects is negligeable, since $\dot{M}(M)$ is modified by less than 2%. The 10% more deuterium allowed in the lower metallicity grid adds approximately 1.6 $L_\odot$ to the nuclear luminosity when deuterium burns at its equilibrium value ($L_{\rm eq} = \epsilon\dot{M}$, where ϵ is the amount of energy available in deuterium per unit mass of accreted material). The increased nuclear flux is however effectively counteracted by the decreased interior opacity. As a result, though defining a larger area in the HRD, the birthline joins the ZAMS earlier at $Z = 0.001$. Indeed, the two birthlines superimpose nearly perfectly at least until the end of the thermal relaxation process, and the larger area in the HRD accessible to the pre-MS evolution is

Table 1. Birthline features at $Z = 0.020$. For each model we give its age, mass, surface luminosity, effective temperature, radius, total gravitational luminosity, total nuclear luminosity, convective core extension (in mass fraction), temperature at the bottom of the convective envelope, depth of the convective envelope (in mass fraction) and relative deuterium surface abundance, respectively. The age of the 0.7 $M_\odot$ starting core was corrected by the amount $0.7\dot{M}^{-1}$, since $\dot{M}(< 0.7) \simeq$ const $\simeq 10^{-5}$ $M_\odot$ yr^{-1}

NB	Age yr	Mass $M_\odot$	Log$L$ $L_\odot$	LogT_e K	R $R_\odot$	L_{grav} $L\odot$	L_{nucl} $L\odot$	M_{core} $M/M_\odot$	LogT_b K	M_{env} $M/M_\odot$	$^2H_{surf}$ $^2H_{IM}$
1	7.923E+04	0.801	0.731	3.632	4.223	-16.79	22.17	1.000	6.177	1.000	6.832E-02
2	8.826E+04	0.901	0.781	3.640	4.311	-15.01	21.05	1.000	6.216	1.000	2.134E-02
3	9.718E+04	1.000	0.813	3.647	4.331	-11.05	17.55	1.000	6.260	1.000	6.056E-03
4	1.192E+05	1.250	0.856	3.662	4.247	-10.35	17.53	1.000	6.363	1.000	1.457E-03
5	1.406E+05	1.500	0.875	3.673	4.126	-10.46	17.96	1.000	6.453	1.000	9.329E-04
6	1.572E+05	1.700	0.883	3.680	4.033	-10.74	18.38	1.000	6.516	1.000	8.565E-04
7	1.815E+05	2.000	0.903	3.692	3.905	-10.97	18.97	1.000	6.600	1.000	8.624E-04
8	2.201E+05	2.500	0.922	3.708	3.708	-11.60	19.95	0.000	6.578	0.750	2.205E-03
9	2.568E+05	3.000	0.962	3.723	3.623	-11.01	20.17	0.000	6.410	0.291	6.165E-03
10	2.929E+05	3.519	1.046	3.739	3.708	-13.85	24.96	0.000	6.304	0.118	1.478E-02
11	3.250E+05	4.001	1.236	3.760	4.189	-7.25	24.45	0.000	6.090	0.022	1.363E-01
12	3.573E+05	4.508	2.294	3.933	6.383	187.84	8.68	0.000	6.092	0.000	1.000E+00
13	3.875E+05	5.001	2.781	4.062	6.173	599.89	3.07	0.000	6.176	0.000	1.000E+00
14	4.171E+05	5.504	3.107	4.185	5.100	1266.04	11.02	0.000	6.262	0.000	1.000E+00
15	4.457E+05	6.006	3.238	4.278	3.864	-142.26	1868.80	0.220	6.200	0.000	1.000E+00
16	4.735E+05	6.515	3.117	4.276	3.393	-702.63	2009.42	0.342	6.203	0.000	1.000E+00
17	4.994E+05	7.001	3.265	4.315	3.362	497.19	1340.07	0.236	6.203	0.000	1.000E+00
18	5.254E+05	7.506	3.295	4.328	3.278	-3815.43	5784.05	0.450	6.191	0.000	1.000E+00
19	5.507E+05	8.013	3.468	4.365	3.374	-539.89	3471.59	0.307	6.209	0.000	1.000E+00

Table 2. Same as Table 1 for $Z = 0.001$

NB	Age yr	Mass $M_\odot$	Log$L$ $L_\odot$	LogT_e K	R $R_\odot$	L_{grav} $L\odot$	L_{nucl} $L\odot$	M_{core} $M/M_\odot$	LogT_b K	M_{env} $M/M_\odot$	$^2H_{surf}$ $^2H_{IM}$
1	7.859E+04	0.800	0.889	3.685	3.968	-19.21	26.95	1.000	6.178	1.000	5.626E-02
2	8.705E+04	0.900	0.929	3.692	4.023	-14.77	23.25	1.000	6.220	1.000	1.519E-02
3	9.548E+04	1.000	0.950	3.697	4.028	-11.89	20.80	1.000	6.266	1.000	5.491E-03
4	1.162E+05	1.250	0.975	3.709	3.923	-11.38	20.82	1.000	6.371	1.000	1.623E-03
5	1.363E+05	1.500	0.993	3.720	3.807	-11.38	21.22	1.000	6.461	1.000	1.111E-03
6	1.521E+05	1.700	0.998	3.726	3.725	-11.72	21.67	1.000	6.525	1.000	9.209E-04
7	1.751E+05	2.001	1.003	3.735	3.594	-12.10	22.17	0.000	6.418	0.649	1.733E-03
8	2.118E+05	2.500	1.078	3.750	3.657	-9.57	21.53	0.000	6.248	0.203	3.218E-02
9	2.468E+05	3.001	1.287	3.770	4.242	6.88	12.47	0.000	5.984	0.025	9.710E-01
10	2.814E+05	3.519	2.241	3.933	6.005	166.28	7.67	0.000	5.993	0.000	1.000E+00
11	3.120E+05	4.000	2.587	4.051	5.195	382.08	3.71	0.000	6.051	0.000	1.000E+00
12	3.427E+05	4.501	2.832	4.160	4.169	678.67	-0.59	0.000	6.083	0.000	1.000E+00
13	3.721E+05	5.001	3.015	4.255	3.324	984.45	48.87	0.000	6.037	0.000	1.000E+00
14	4.010E+05	5.510	3.149	4.336	2.671	1111.81	294.88	0.000	6.107	0.000	1.000E+00
15	4.281E+05	6.005	3.235	4.393	2.268	327.30	1387.36	0.127	6.236	0.000	1.000E+00
16	4.544E+05	6.502	3.217	4.404	2.112	-1620.31	3265.38	0.396	6.242	0.000	1.000E+00
17	4.801E+05	7.002	3.212	4.400	2.139	-1682.74	3308.98	0.409	6.233	0.000	1.000E+00
18	5.054E+05	7.511	3.310	4.412	2.265	-1646.97	3684.76	0.392	6.226	0.000	1.000E+00
19	5.292E+05	8.002	3.411	4.425	2.397	-1689.52	4260.70	0.385	6.223	0.000	1.000E+00

actually the result of the shift of the ZAMS to higher effective temperatures when lowering the metallicity.

By virtue of the huge radiative flux delivered by deuterium burning, which amplifies convective instability, the temperatures reached at the bottom of the convective envelope are high enough to modify the surface abundances of both isotopes of lithium. For example, at Z=0.020 the more fragile ^{6}Li shows a deep near 2.45 $M_\odot$ ($T_{\rm eff} \approx$ 5000 K) at nearly half its ISM content, increases again at successive stages being simply diluted, and then goes back to its original value a little before the convective envelope disappears. A similar, though softer trend, is also apparent in the ^{7}Li surface abundance. We will show in a subsequent paper, however, that this result is subordinated to the artificial way the newly added deuterium is instantaneously mixed (an invalid hypothesis, indeed), and how a diffusive approach to its destruction can effectively prevent the present outcome.

The pre-MS evolution: Models on the birthline become the starting configurations for the following quasi-static contraction at constant mass once accretion is halted (here abruptly), and the stars become optically visible. This part of the evolution of a young star is entirely dominated by gravity, which is by far its only source of luminosity. In speaking about this stage, that is from the birthline to the ZAMS, we will refer to *pre-MS contraction time* $t_{\rm PMS}$ and *pre-MS evolution*, to distinguish them from the *total youth time* $t_{\rm you}$ which also adds to the pre-MS phase the time spent by an accreting protostars hidden behind its dusty parental cocoon.

Pre-MS evolutionary tracks for both metallicities in the mass range 0.8−5 $M_\odot$ are displayed in Fig. 1. Some salient characteristics of these numerical solutions are collected in Tables 3 and 4, where the new $t_{\rm PMS}$ (together with $t_{\rm you}$) are compared to the canonical contraction times $t_{\rm can}$ of BM. We shall limit our analysis to a few considerations:

- At their first appearence on the birthline, the accretion, partially radiative models differ from a classical configuration evolved at constant mass. Though quasi-statically contracting, they are far from thermal equilibrium. For instance, it takes 5 10^5 yr for a 3 $M_\odot$ of solar metallicity to thermally relax and join its Henyey track. From there on, however, the two scenarios predict strictly the same surface properties;

- Except for two very thin layers in correspondence with the ionization temperatures of hydrogen ($\sim$ 10000 K) and helium ($\sim$ 40000 K), intermediate mass models possess radiative envelopes. The problem may then remain to explain the observed optical activity displayed by Herbig stars, if ascribed to magnetic dynamo action (Boehm & Catala 1993);

- A prominent feature of the accretion models, is to produce a shorter pre-MS phase if compared to standard predictions which usually start arbitrarily high on a luminous Hayashi adiabat. For a 5 $M_\odot$ model, $t_{\rm PMS}$ is reduced to nearly 30% of the value one would have expected otherwise. At solar or subsolar masses, $t_{\rm can}$ and $t_{\rm PMS}$ are sensibly the same, however. A different trend is shown by the youth time which, once the ZAMS has been reached, becomes higher than the canonical contraction time and slightly increases with respect to the hydrogen burning timescale, too.

- We recover in the ZAMS surface abundances of lithium (between 2−3 $M_\odot$) the effects leftover by mixing in the convective portion of the accretion period. We recall that a fully diffusive treatment of deuterium burning would erase these local minima. Otherwise, the depletion levels are a well known consequence of the deeper, hotter and more lasting convective envelopes possessed by lower mass pre-MS stars.

Table 3. Time intervals (in unit of 10^6 yr) and ^{7}Li relative surface abundance of ZAMS models for $Z = 0.020$. Contraction times are fixed by the last minimum total radius prior to the hydrogen supported burning stage (cf. text for the definition of the various quantities). Note that $t_{\rm PMS} = t_{\rm you}$(col4/ col3)

Final mass	Youth time	$\frac{t_{\rm you}}{t_{\rm can}}$ [1]	$\frac{t_{\rm PMS}}{t_{\rm can}}$ [1]	$\frac{t_{\rm acc}}{t_{\rm H}}$ [2]	$\frac{^7{\rm Li_s}}{^7{\rm Li_0}}$
$5M_\odot$	0.799	0.694	0.358	0.0085	1.000
4	1.414			0.0086	1.000
3	2.683	0.371	0.335	0.0076	0.993
2.5	4.631			0.0079	0.977
2	11.72	0.501	0.493	0.0105	0.999
1.7	14.61			0.0799	0.990
1.5	30.95	0.874	0.870	0.0115	0.958
1.25	36.18			0.0074	0.776
1	38.21	0.982	0.978	0.0038	0.199
0.9	50.42			0.0033	0.029
0.8	71.54	1.045	1.044	0.0028	0.000

[1] $t_{\rm can}$ are from Bernasconi & Maeder 1996
[2] $t_{\rm H}$ are from Schaller et al. 1992

A. Tables retrieval by remote file-transfer

The results published in this work, with more complete tables for birthlines and pre-MS stellar tracks, are available by anonymous file-transfer (ftp). For a description of the procedure contact the author by electronic mail, or directly access to the Geneva Stellar Evolution Database at the WWW site http://obswww.unige.ch/schaerer/evol/Welcome.html.

References

Basri G., Martín E.L., Bertout C., 1991, A&A 252, 625
Bernasconi P.A., Maeder A., 1996, A&A 307, 829 (BM)
Boehm T., Catala C., 1993, A&AS 101, 629
Boesgaard A.M., Steigman G., 1985, ARA&A 23, 319

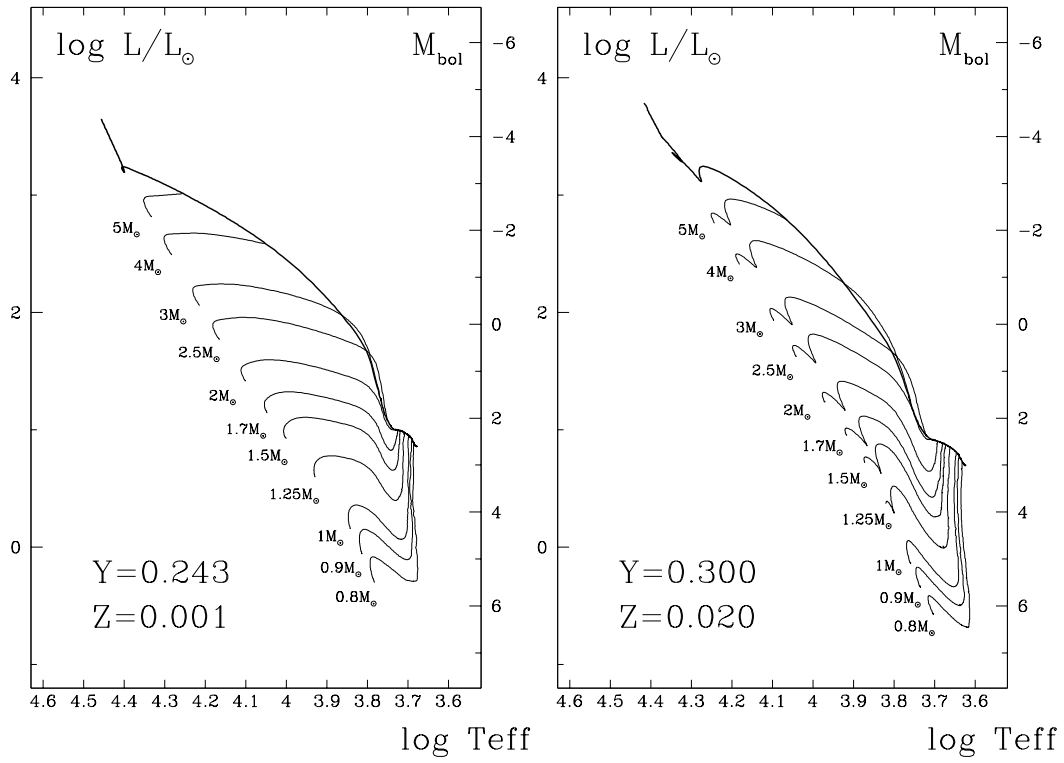

Fig. 1. Theoretical HR diagrams for the computed pre-MS models in the accretion paradigm for star formation at metallicities $Z = 0.001$ and $Z = 0.020$. Thick lines mark the evolutionary path followed by the accreting core in the turbulent solution of BM for isolated massive stars. Near the ZAMS, the effects of the out-equilibrium CNO burning are too small to be observable in the lower metallicity grid

Table 4. Same as Table 3 for $Z = 0.001$

Final mass	Youth time	$\frac{t_{\rm you}}{t_{\rm can}}$ [1]	$\frac{t_{\rm PMS}}{t_{\rm can}}$ [1]	$\frac{t_{\rm acc}}{t_{\rm H}}$ [2]	$\frac{^7{\rm Li_s}}{^7{\rm Li_0}}$
$5M_\odot$	0.585	1.114	0.406	0.0066	1.000
4	0.807			0.0056	1.000
3	1.415	0.852	0.704	0.0049	1.000
2.5	2.290			0.0047	1.000
2	4.224	0.928	0.890	0.0049	0.999
1.7	6.464			0.0049	1.000
1.5	9.384	0.868	0.855	0.0051	1.000
1.25	14.89			0.0046	1.000
1	22.49	1.092	1.087	0.0036	0.999
0.9	27.59			0.0029	0.997
0.8	37.14	1.012	1.010	0.0025	0.990

[1] $t_{\rm can}$ are from Bernasconi & Maeder 1996
[2] $t_{\rm H}$ are from Schaller et al. 1992

Bouvier J., Cabrit S., Fernández M., Martín E.L., Matthews J.M., 1993, A&A 272, 176
Geiss J., 1993, Origin and Evolution of the Elements. In: Pantzos N., Vangioni-Flam E., Cassé M. (eds.). Cambridge Univ. Press, p. 89
Iglesias C.A., Rogers F.J., 1993, ApJ 412, 752
Iglesias C.A., Rogers F.J., Wilson B.G., 1992, ApJ 397, 717
Kurucz R.L., 1991, in Stellar Atmospheres: Beyond Classical Models, NATO ASI Series C, Vol. 341. In: Crivellari L., Hubeny I., Hummer D.G. (eds.), p. 441
Larson R.B., 1969, MNRAS 145, 271
Larson R.B., 1981, MNRAS 194, 809
Martin E.L., Claret A., 1996, A&A, (in press)
Mercer-Smith J.A., Cameron A.G.W., Epstein R.I., 1984, ApJ 279, 363
Palla F., 1996, SOC Workshop 1995
Palla F., Stahler S.W., 1991, ApJ 375, 288; 1993, ApJ 418, 414
Palla F., Stahler S.W., 1992, ApJ 392, 667
Schaller G., Schaerer D., Meynet G., Maeder A., 1992, A&AS 96, 269
Stahler S.W., 1983, ApJ 274, 822
Tscharnuter W.M., 1991, The Physics of Star Formation and Early Stellar Evolution. In: Lada C.J. and Kylafis N.D. (eds.), NATO ASI Series Vol. 342, p. 411